

## $^{13}\text{C}\text{I}$ in high-mass star-forming clouds

A. R. Tieftrunk<sup>1</sup>, K. Jacobs<sup>1</sup>, C. L. Martin<sup>2</sup>, O. Siebertz<sup>1</sup>,  
A. A. Stark<sup>2</sup>, J. Stutzki<sup>1</sup>, C. K. Walker<sup>3</sup>, and G. A. Wright<sup>4</sup>

<sup>1</sup> KOSMA, I. Physikalisches Institut der Universität Köln, Zùlpicher Str. 77, 50937 Köln, Germany

<sup>2</sup> Smithsonian Astrophysical Observatory, 60 Garden Street, Cambridge MA 02138, USA

<sup>3</sup> Steward Observatory, University of Arizona, Tucson AZ 85721, USA

<sup>4</sup> Bell Laboratories, 791 Holmdel-Keyport Rd., Holmdel NJ 07733, USA

Received 11 May 2001 / Accepted 2 June 2001

**Abstract.** We report measurements of the  $^{12}\text{C}/^{13}\text{C}$  abundance ratio in the three galactic regions G 333.0-0.4, NGC 6334 A and G 351.6-1.3 from observations of the  $^{12}\text{C}\text{I } ^3P_2 \rightarrow ^3P_1$  transition and the hyperfine components of the corresponding  $^{13}\text{C}\text{I}$  transition near 809 GHz. These transitions were observed simultaneously with the CO 7–6 line emission at 806 GHz with the AST/RO telescope located at the South Pole. From a simultaneous fit to the  $^{12}\text{C}\text{I } ^3P_2 \rightarrow ^3P_1$  transition and the HF components of the corresponding  $^{13}\text{C}\text{I}$  transition and an independent estimate of an upper limit to the optical depth of the  $^{12}\text{C}\text{I}$  emission we determine intrinsic  $^{12}\text{C}\text{I}/^{13}\text{C}\text{I}$  column density ratios of  $23 \pm 1$  for G 333.0-0.4,  $56 \pm 14$  for NGC 6334 A and  $69 \pm 12$  for G 351.6-1.3. As the regions observed are photon dominated, we argue that the apparent enhancement in the abundance of  $^{13}\text{C}$  towards G 333.0-0.4 may be due to strong isotope-selective photodissociation of  $^{13}\text{CO}$ , outweighing the effects of chemical isotopic fractionation as suggested by models of PDRs. Towards NGC 6334 A and G 351.6-1.3 these effects appear to be balanced, similar to the situation for the Orion Bar region observed by Keene et al. (1998).

**Key words.** ISM: abundances – atoms – clouds – H II regions – submillimeter

### 1. Introduction

The study of CNO isotope abundance ratios in the interstellar medium is crucial to understanding galactic chemical evolution. In particular, the ubiquity of C-based molecules in interstellar clouds has made the  $^{12}\text{C}/^{13}\text{C}$  abundance ratio an important chemical diagnostic. From measurements of  $\text{C}^{18}\text{O}$  and  $^{13}\text{C}^{18}\text{O}$  in 13 interstellar clouds, Langer & Penzias (1990, 1993) found a galactic gradient in the local carbon isotope abundance ratio (hereafter:  $n(\text{C})$ -ratio) ranging from 25 towards the galactic center to about 60–70 in the local ISM and out to a galactic radius of about 10 kpc. They also found an increase in the  $n(\text{C})$ -ratio derived from CO towards clouds exposed to higher UV radiation fields (namely Orion KL and W33), supporting the suggestion made by models of photon dominated regions (PDRs) that depletion in  $^{13}\text{CO}$  can be ascribed to inefficient self-shielding resulting in isotope-selective photodissociation (van Dishoeck & Black 1988).

As discussed by Keene et al. (1998), who report the first detection of the strongest of the  $^{13}\text{C}\text{I}$  hyperfine (HF) structure components at 809 GHz from the Orion Bar region, the abundance of atomic carbon is sensitive to the effects of chemical isotopic fractionation and isotope-

selective photodissociation, allowing the study of the significance of these competing effects in PDRs and to verify model predictions (e.g. Le Bourlot et al. 1993; Köster et al. 1994). The charge exchange fractionation reaction,  $^{13}\text{C}^+ + ^{12}\text{CO} \rightleftharpoons ^{12}\text{C}^+ + ^{13}\text{CO} + 36 \text{ K}$ , being exothermic, preferentially incorporates  $^{13}\text{C}^+$  into  $^{13}\text{CO}$ , thus leading to a local  $^{13}\text{C}^+$  and  $^{13}\text{C}\text{I}$  depletion and a corresponding  $^{13}\text{CO}$  enhancement. This may be balanced by isotope-selective photodissociation, which in contrast reduces the gas-phase abundance of the less efficiently self-shielded  $^{13}\text{CO}$  isotopomer (van Dishoeck & Black 1988). Models show that the proportion of these effects strongly depends on the temperature derived for the  $\text{C}^+/\text{C}\text{I}/\text{CO}$  transition zone (due to the low energy barrier of the exchange reaction) and the comparison between different models gives non-conclusive results (Köster et al. 1994; Le Bourlot et al. 1993).

From their measurement of the  $^{12}\text{C}\text{I } ^3P_2 \rightarrow ^3P_1$  and the strongest HF component of the  $^{13}\text{C}\text{I}$  equivalent transition, Keene et al. (1998) find a  $N(^{12}\text{C})/N(^{13}\text{C})$  column density ratio (hereafter:  $N(\text{C})$ -ratio) of  $58 \pm 12$  towards a position near the western end of the Orion bar. They derive a somewhat higher ratio of  $75 \pm 9$  towards the same position from observations of  $\text{C}^{18}\text{O}$  and  $^{13}\text{C}^{18}\text{O}$ . In comparison, direct observations of the  $^{12}\text{C}^+ / ^{13}\text{C}^+$  abundance ratio (Stacey et al. 1993; Boreiko & Betz 1996), which should not be significantly influenced by chemical

isotopic fractionation or isotope-selective photodissociation, yield a  $n(\text{C})$ -ratio of  $58 \pm 6$ . Keene et al. (1998) conclude that, in contrast to the model results by Le Boulout et al. (1993) the importance of chemical isotopic fractionation is (almost) compensated for by the isotope-selective photodissociation. Whether this compensation is peculiar to the special conditions of the Orion Bar, or whether it also holds for other massive star-forming cores is a significant question when addressing galactic chemical evolution, since our current understanding is almost entirely based on the observed carbon monoxide isotopomer abundance ratios. It is therefore important to extend the study of  $^{13}\text{C}$  to other regions.

In this Letter, we report measurements of the  $^3P_2 \rightarrow ^3P_1$  transition of  $^{12}\text{C}$  at 809341.97 MHz and the  $F = 5/2-3/2$ ,  $F = 3/2-1/2$ , and  $F = 3/2-3/2$  components of the equivalent transition of  $^{13}\text{C}$  at 809493.7 MHz, 809125.5 MHz, and 809121.3 MHz, respectively, towards three galactic star-forming regions associated with strong IRAS sources and CO emission: G 333.0-0.4, part of the large H II complex RCW 106 and associated with a molecular cloud with bright CO lines (Gillespie et al. 1977; Brand et al. 1984) at a distance of 4.2 kpc (Shaver & Goss 1970); NGC 6334 A, a bright FIR continuum region (McBreen et al. 1973) associated with a bright PDR (Burton et al. 2000; Kraemer et al. 2000) located within a giant molecular cloud at a distance of 1.7 kpc (Neckel 1978); and G 351.6-1.3, a luminous ( $L_{\text{bol}} \approx 10^6 L_{\odot}$ ) compact H II region excited by an embedded O/B cluster (McBreen et al. 1983) at a distance of 5 kpc (Radhakrishnan et al. 1973). These regions were selected because of strong emission in the  $^3P_1 \rightarrow ^3P_0$  transition of  $^{12}\text{C}$  at 492 GHz (Huang et al. 1999) from a list of 30 candidates of galactic H II regions having strong CO (Brand et al. 1984; Henning & Launhardt 1998) and CS (Bronfman et al. 1996; Launhardt et al. 1998) emission lines.

## 2. Observations

The observations were made in the Austral winter of 2000 with the 800 GHz receiver at the Antarctic Submillimeter Telescope and Remote Observatory (AST/RO, cf. Stark et al. 2001). At these frequencies the FWHM beam size is  $\approx 80''$ . As backend we used an AOS with a velocity resolution of  $0.25 \text{ km s}^{-1}$  at the observed frequencies. The zenith opacities at 809 GHz at the times of observation were  $\approx 1.0 \pm 0.2$ . System temperatures on average were between 11 000 K for G 333.0-0.4, 18 000 K for NGC 6334 A, and 25 000 K for G 351.6-1.3. The  $^{12}\text{C}$  and  $^{13}\text{C}$  lines were observed in the lower sideband simultaneously with the CO 7-6 line in the upper sideband. The spectra were calibrated (Stark et al. 2001) to the effective radiation temperature  $T_{\text{R}}^*$  scale. The frequencies reported by Klein et al. (1998) (cf. Cologne Database for Molecular Spectroscopy – [www.cdms.de](http://www.cdms.de)) were used to determine the line centroids.

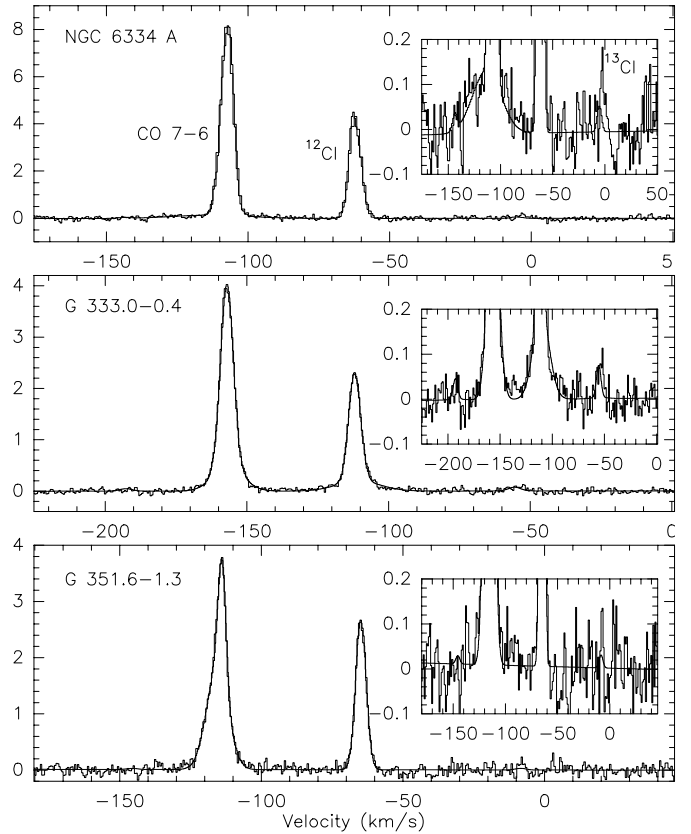


**Fig. 1.** Broad band spectra (50 hrs of integration time on source) towards the galactic star-forming regions NGC 6334 A (top), G 333.0-0.4 (middle) and G 351.6-1.3 (bottom). The insets show the same spectra magnified in  $y$ -scale. The  $^{12}\text{C}$  and  $^{13}\text{C}$  lines were observed in the lower sideband simultaneously with the CO 7-6 line in the upper sideband. Note the erratic baseline toward the  $^{13}\text{C}$  line emission in G 351.6-1.3, which resulted in a skewed baseline fit and precludes a clear  $3\sigma$  assignment of this peak.

## 3. Results

Figure 1 shows the spectra obtained towards the three regions. The strongest HF component of  $^{13}\text{C}$  at 809 GHz,  $F = 5/2-3/2$ , is clearly visible in the G 333.0-0.4 and NGC 6334 A spectra; it is marginally detected in G 351.6-1.3. The weaker HF structure satellites,  $F = 3/2-1/2$  and  $F = 3/2-3/2$ , are still hidden in the noise in all cases. Following the first detection towards Orion by Keene et al. (1998), these regions are the only other  $^{13}\text{C}$  detections to date. We derive the  $^{12}\text{C}/^{13}\text{C}$  intensity ratio by a simultaneous Gaussian fit of the lines (including all  $^{13}\text{C}$  HF components) with *fixed spacing and a single line width*, and with the ratio of the  $^{13}\text{C}$  amplitudes fixed to their quantum mechanical values of 0.600:0.333:0.067; the free fit parameters are the common width and LSR-velocity, a common amplitude and the relative line intensity ratio  $\alpha = \frac{I_{12}}{I_{13}}$ . We included the CO 7-6 line from the other sideband as an additional, independent Gaussian. Due to broad line wings apparent in the CO and  $^{12}\text{C}$  emission lines towards G 333.0-0.4, we fit two line components (broad & narrow) for all emission lines here.

**Table 1.** Line fit results.

emission line	$T_{\text{R}}^*$ [K]	$\Delta v_{\text{lsr}}$ [km s $^{-1}$ ]	$\alpha$ $\frac{I_{12}}{I_{13}}$	
NGC 6334 A				
$^{13}\text{C I}$	$0.10 \pm 0.02$	$4.9 \pm 0.2$	$45 \pm 11$	n
CO	$8.04 \pm 0.06$	$5.3 \pm 0.1$		n
CO	$0.14 \pm 0.03$	$32 \pm 7$		b
G 333.0-0.4				
$^{13}\text{C I}$	$0.12 \pm 0.02$	$5.0 \pm 0.1$	$18 \pm 1$	narrow
$^{13}\text{C I}$	$0.04 \pm 0.01$	$18 \pm 1$	$45 \pm 4$	broad
CO	$3.57 \pm 0.02$	$5.4 \pm 0.1$		n
CO	$0.46 \pm 0.02$	$12.6 \pm 0.4$		b
G 351.6-1.3				
$^{13}\text{C I}$	$0.05 \pm 0.01$	$4.4 \pm 0.1$	$55 \pm 10$	n
CO	$2.15 \pm 0.02$	$3.3 \pm 0.1$		n
CO	$1.77 \pm 0.02$	$8.9 \pm 0.2$		b

The  $^{13}\text{C I}$  amplitudes given are the sum over the three HF components (see text).

In the case of NGC 6334 A and G 351.6-1.4, where no wings are apparent for the  $^{12}\text{C I}$  line but asymmetric line profiles are conspicuous for the CO 7–6 line, we fit a second broad line component to the CO emission line only. The fit results for all sources are given in Table 1. The uncertainties quoted are the formal fit errors based on a  $1\sigma$  excursion. Since the  $^{13}\text{C I}$  and  $^{12}\text{C I}$  lines were measured simultaneously in the same receiver sideband, calibration uncertainties are negligible.

In the optically thin case, the  $N(\text{C})$ -ratio is directly given by the line intensity ratio  $\alpha$ ; beyond this limit an optical depth correction must be applied. We prefer this approach to the alternative of including the optical depth into the fit by fitting saturated line profiles of the form  $1 - \exp(-\tau \times \phi_\nu)$ , because of the macro-turbulent nature of the velocity field in the ISM and the corresponding failure to observe saturated profiles even for optically thick lines of  $^{13}\text{CO}$  in any astronomical source. This is supported by the Gaussian profile fit to the CO 7–6 line with a width only marginally wider than that of  $^{12}\text{C I}$ .

### 3.1. Optical depth estimate

To derive the intrinsic  $^{12}\text{C I}/^{13}\text{C I}$  column density ratio,  $N(\text{C})$ , we apply an optical depth correction to  $\alpha$ . Following Keene et al. (1998), the ratio is given by

$$\frac{N(^{12}\text{C})}{N(^{13}\text{C})} = \frac{\alpha}{\beta(\tau_{12\text{C}})}, \quad (1)$$

with the line escape probability  $\beta(\tau) = (1 - e^{-\tau})/\tau$ . To further constrain the properties of the C I emitting gas, we use the line intensity ratio of the  $^{12}\text{C I } ^3P_2 \rightarrow ^3P_1$  and  $^3P_1 \rightarrow ^3P_0$  emission lines. The 492 GHz  $^{12}\text{C I } ^3P_1 \rightarrow ^3P_0$  line transition has also been measured (Huang et al. 1999) towards these sources; assuming that the emission is extended and need not be corrected for different beam sizes

at 492 and 809 GHz, we derive a line intensity ratio of 0.48 for G 333.0-0.4, 0.63 for NGC 6334, and 0.75 for G 351.6-1.4. If the sources are centrally peaked, coupling to the narrower 809 GHz beam would be higher, and the intrinsic line ratios would be correspondingly lower.

We use a single component escape probability excitation code (Stutzki & Winnewisser 1985) to interpret the observed line intensities. As an additional constraint we need an estimate of the source density. Only for NGC 6334 do we have an estimate: Kraemer et al. (1998) compared their observed line intensities of C II (158  $\mu\text{m}$ ) and O I (146  $\mu\text{m}$  & 63  $\mu\text{m}$ ) and the CO line and FIR continuum intensities to PDR models of Wolfire et al. (1990) to estimate the gas density and FUV field towards the embedded radio continuum sources. Towards NGC 6334 A they derive an average FUV field of  $\log G_0 = 4.5$  and a total gas density of  $n(\text{H}_2) = 6.3 \times 10^3 \text{ cm}^{-3}$  within their  $1'$  beam. It is fair to assume that the density of the C I emitting gas in NGC 6334 A and the other two sources is similar or higher, as it is located deeper in the molecular cloud. Densities of that magnitude are also supported by the bright CO 7–6 emissions we observe.

As is shown in Fig. 2, this density immediately constrains the temperature of the C I emitting region to about 40 K or lower: at higher temperatures, the  $^{12}\text{C I } ^3P_2 \rightarrow ^3P_1 / ^3P_1 \rightarrow ^3P_0$  line ratio at these densities would be substantially higher than observed. This temperature estimate is perfectly consistent with the scenario of extended PDR emission. In this regime of density and temperature, the observed  $^{12}\text{C I } ^3P_2 \rightarrow ^3P_1 / ^3P_1 \rightarrow ^3P_0$  line ratio constrains the column density per unit velocity interval to values below  $2 \times 10^{17} \text{ cm}^{-2} / \text{km s}^{-1}$  and corresponding optical depths of the  $^{12}\text{C I } ^3P_2 \rightarrow ^3P_1$  line below  $\tau \approx 0.4$ . At higher column densities trapping would push the line ratio to much higher values than observed.

The total column density in the  $\approx 5 \text{ km s}^{-1}$  wide  $^{12}\text{C I}$  lines is then about  $10^{18} \text{ cm}^{-2}$ ; this corresponds, with the standard gas phase abundance of carbon of about  $10^{-4}$ , to a hydrogen column density of  $10^{22} \text{ cm}^{-2}$ . Considering that each PDR surface has a C I column density corresponding to an  $A_V$  of a few, we therefore conclude that we see a few PDR surfaces per beam, consistent with the usual scenario of a clumpy, UV-penetrated massive cloud core.

## 4. Discussion

For the range of density, temperature and column density derived above, our radiative transfer model predicts line brightnesses for the  $^{12}\text{C I } ^3P_2 \rightarrow ^3P_1$  lines of around 5–10 K. Since the measured line brightnesses are a few degrees in the observed sources, we estimate a beam filling factor close to unity, consistent with extended, smooth emission within the AST/RO beam. This scenario suggests the  $^{12}\text{C I}$  emission is moderately optically thin. For the rough upper limit of the optical depth  $\tau \approx 0.4$ , the optical depth correction factor  $1/\beta(\tau) = 1.21$  only raises the  $N(\text{C})$ -ratio derived above by at most 25%. We estimate

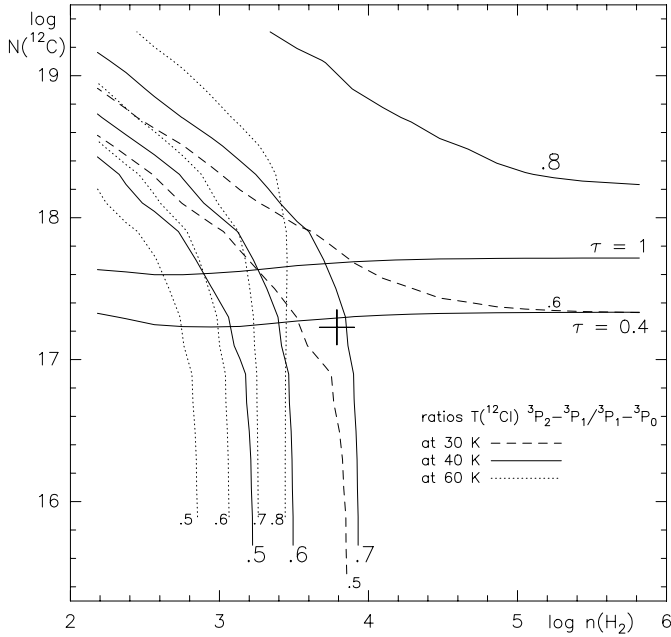


**Fig. 2.** Results from the line escape probability code: Bold lines show  $^{12}\text{C}$  line ratios for 40 K. At these temperatures and lower (30 K, dashed), densities of  $n(\text{H}_2) = 6.3 \times 10^3 \text{ cm}^{-3}$  indicate an optical depth of  $\tau < 0.4$  and constrain the densities to  $N(^{12}\text{C}) < 2 \times 10^{17} \text{ cm}^{-2}/\text{km s}^{-1}$  (indicated by a cross). At higher temperatures (60 K, dotted) the ratios at these densities would be substantially higher than observed.

the  $N(\text{C})$ -ratio in G 333.0-0.4 to be  $23 \pm 1$  or lower ( $56 \pm 5$  for the weak extended component), that in NGC 6334 A to be  $56 \pm 14$  or lower, and that in G 351.6-0.4 to be  $69 \pm 12$  or lower.

The  $N(\text{C})$ -ratios towards G 351.6-1.4 and NGC 6334 A are consistent with the intrinsic isotopic ratios and do not call for significant isotopic fractionation or isotope-selective photodissociation. These results confirm the conclusion of Keene et al. (1998) for their Orion Bar data. Towards G 333.0-0.4, however, we find the ratio to be substantially lower than the average values derived from CO isotopomers. In this context one should recall, that (Langer & Penzias 1993) find an increase in the CO/ $^{13}\text{CO}$ -isotopomer ratio towards clouds exposed to higher UV radiation fields, supporting the suggestion of PDR models that the depletion in  $^{13}\text{CO}$  can be ascribed to less effective self-shielding and enhanced isotope-selective photodissociation (van Dishoeck & Black 1988). This would then yield an increase in the abundance of the  $^{13}\text{C}$  isotope, as is shown in the PDR-models by Köster et al. (1994), if not counter-balanced by chemical isotopic fractionation. As chemical isotopic fractionation becomes more efficient with decreasing temperatures and eventually dominates over isotope-selective photodissociation, there will be a decrease in the abundance of the  $^{13}\text{C}$  isotope. This is shown in the PDR models of Le Bourlot et al. (1993), which produce a lower temperature in the transition zone due to reduced heating. Cloud surface temperatures therefore influence the balance of the two competing effects and,

ultimately, determine the carbon isotope abundance ratio. The temperature structure in PDR surfaces, details of which are not consistently explained by present PDR models, might be responsible for the very different atomic carbon isotope abundance ratios observed to date.

*Acknowledgements.* The Letter is dedicated to Rodney Marks, who was working as the Winterover Scientist for the AST/RO project when he died on May 12th, 2000, during preparations for these observations. The CARA winter-over crew, Gene Davidson, Greg Griffin, David Pernic, and John Yamasaki, continued AST/RO operations in tribute to Rodney's memory, allowing these observations to be made. The Universität Köln contribution to AST/RO was supported by special funding from the Science Ministry of the Land Nordrhein-Westfalen and by the Deutsche Forschungsgemeinschaft through grant SFB 301. This work was supported in part by United States National Science Foundation grant DPP88-18384, and by the Center for Astrophysical Research in Antarctica (CARA) and the NSF under Cooperative Agreement OPP89-20223.

## References

- Boreiko, R. T., & Betz, A. L. 1996, *ApJ*, 467, L113  
 Brand, J., van der Bij, M. D. P., de Vries, C. P., et al. 1984, *A&A*, 139, 181  
 Bronfman, L., Nyman, L.-A., & May, J. 1996, *A&AS*, 115, 81  
 Burton, M. G., Ashley, M. C. B., Marks, R. D., et al. 2000, *ApJ*, 542, 359  
 Gillespie, A. R., Huggins, P. J., Sollner, T. C. L. G., et al. 1977, *A&A*, 60, 221  
 Henning, T., & Launhardt, R. 1998, *A&A*, 338, 223  
 Huang, M., Bania, T. M., Bolatto, A., et al. 1999, *ApJ*, 517, 288  
 Keene, J., Schilke, P., Kooi, J., et al. 1998, *ApJ*, 494, L107  
 Klein, H., Lewen, F., Schieder, R., Stutzki, J., & Winnewisser, G. 1998, *ApJ*, 494, L125  
 Köster, B., Störzer, H., Stutzki, J., & Sternberg, A. 1994, *A&A*, 284, 545  
 Kraemer, K. E., Jackson, J. M., & Lane, A. P. 1998, *ApJ*, 503, 785  
 Kraemer, K. E., Jackson, J. M., Lane, A. P., & Paglione, T. A. D. 2000, *ApJ*, 542, 946  
 Langer, W. D., & Penzias, A. A. 1990, *ApJ*, 357, 477  
 Langer, W. D., & Penzias, A. A. 1993, *ApJ*, 408, 539  
 Launhardt, R., Evans, N. J. I., Wang, Y., et al. 1998, *ApJS*, 119, 59  
 Le Bourlot, J., Pineau des Fôrets, G., Roueff, E., & Flower, D. R. 1993, *A&A*, 267, 233  
 McBreen, B., Fazio, G. G., Stier, M., & Wright, E. L. 1973, *ApJ*, 232, L183  
 McBreen, B., Loughran, L., Fazio, G. G., & Rengarajan, T. N. 1983, *AJ*, 90, 88  
 Neckel, T. 1978, *A&A*, 69, 51  
 Radhakrishnan, V., Goss, W. M., Murray, J. D., & Brooks, J. W. 1973, *ApJS*, 24, 49  
 Shaver, P. A., & Goss, W. M. 1970, *AuJPA*, 14  
 Stacey, G. J., Jaffe, D. T., Geis, N., et al. 1993, *ApJ*, 404, 219  
 Stark, A. A., Bally, J., Balm, S. P., et al. 2001, *PASP*, 113, 567  
 Stutzki, J., & Winnewisser, G. 1985, *A&A*, 144, 1  
 van Dishoeck, E. F., & Black, J. 1988, *ApJ*, 334, 711  
 Wolfire, M. G., Tielens, A. G. G. M., & Hollenbach, D. 1990, *ApJ*, 358, 116